Published in final edited form as:
Plast Reconstr Surg. 2012 April ; 129(4): 888–896. doi:10.1097/PRS.0b013e3182450ae5.

Metrics of Cellular and Vascular Infiltration of Human Acellular Dermal Matrix in Ventral Hernia Repairs

Kristin Turza Campbell, M.D.[1], **Nadja K. Burns, M.D.**[1], **Joe Ensor, Ph.D.**[2], and **Charles E. Butler, M.D.**[1]

[1]Department of Plastic Surgery, The University of Texas MD Anderson Cancer Center, Houston, TX

[2]Department of Biostatistics, The University of Texas MD Anderson Cancer Center, Houston, TX

Abstract

Background—Human acellular dermal matrix (HADM) is used for ventral hernia repair, as it resists infection and remodels via surrounding tissue. However, the tissue source and impact of basement membrane (BM) on cell and vessel infiltration have not been determined. We hypothesized that musculofascia would be the primary tissue source of cells and vessels infiltrating into HADM and the BM would inhibit infiltration.

Methods—Fifty-six guinea pigs underwent inlay HADM ventral hernia repair with the BM oriented toward or away from the peritoneum. At postoperative weeks 1, 2, or 4, repair sites were completely excised. Histologic and immunohistochemical analyses were performed to quantify cell and vessel density within repair-site zones, including interface (lateral, beneath musculofascia) and center (beneath subcutaneous fat) zones. Cell and vessel quantities were compared as functions of zone, BM orientation, and time.

Results—Cellular and vascular infiltration increased over time universally. The interface demonstrated greater mean cell density than the center (weeks 1 and 2, $p=0.01$, $p<0.0001$). Cell density was greater with the BM oriented toward the peritoneum at week 4 ($p=0.02$). The interface zone had greater mean vessel density than the center zone at week 4 ($p<0.0001$). Orienting the BM toward the peritoneum increased vessel density at week 4 ($p=0.0004$).

Corresponding author: Charles E. Butler, M.D., Department of Plastic Surgery, Unit 1488, The University of Texas MD Anderson Cancer Center, 1515 Holcombe Boulevard, Houston, TX 77030, cbutler@mdanderson.org.

Presentations: This research was presented in part at Plastic Surgery 2010, the 79th annual meeting of the American Society of Plastic Surgeons, Toronto, Canada, October 4, 2010.

Disclosures: Dr. Butler serves as a consultant for LifeCell Corporation.

Products mentioned in manuscript:
AlloDerm (HADM), LifeCell, Branchburg, NJ
Buprenorphine, Bedford Laboratories, Bedford, OH
Ketamine, Fort Dodge Animal Health, Fort Dodge, IA
Xylazine, Vedco Inc., St. Joseph, MO
Isoflurane, Baxter Healthcare, Deerfield, IL
Enrofloxacin, Bayer Health Care, Animal Health Division, Shawnee Mission, KS
Retiga 4000R digital camera, QImaging, Surrey, British Columbia
Olympus IX70 inverted microscope, Olympus, Melville, NY
ImageJ 1.32j software, National Institutes of Health, Bethesda, MD
SAS version 9.2 software, SAS Institute, Cary, NC

Conclusion—Cellular and vascular infiltration into HADM for ventral hernia repairs was greater from musculofascia than subcutaneous and the BM inhibited cellular and vascular. HADM should be placed adjacent to the best vascularizing tissue to improve fibrovascular incorporation.

INTRODUCTION

Bioprosthetic mesh remodeling occurs via cellular and vascular infiltration of the mesh and improves resistance to infection and repair site strength.[1,2] When bioprosthetic mesh is used for ventral hernia repair, there are three potential pathways through which cellular and vascular infiltration of the bioprosthesis can occur: from the peritoneal cavity, from the musculofascial edges, and/or from the subcutaneous fat (in bridged repairs). Although the metrics of vascular in-growth have been established for skin graft–recipient site interfaces,[3] the same has yet to be clearly determined for bioprosthetic mesh in ventral hernia repair.

One form of bioprosthetic mesh commonly used in abdominal wall and breast reconstruction is human acellular dermal matrix (HADM).[4,5,6,7,8,9,10,11,12] Commercially available HADM has two distinct surfaces, one of which contains an intact basement membrane (BM). The natural BM components of skin are intentionally preserved during proprietary HADM processing, including type IV and VII collagen, laminin, and heparan sulfate proteoglycan. In native skin, the BM serves numerous functions including adhering the dermis to the epidermisand providing a mechanical protective barrier, however, the BM may affect the ability of cells or blood vessels to infiltrate into the HADM. Altering the position of the BM during HADM placement-- either toward the peritoneum or the subcutaneous tissue--may influence the quantity and/or speed of recellularization and revascularization.

We hypothesized that cellular and vascular infiltration into HADM would be greater from the musculofascial edge than subcutaneous fat and be inhibited by the BM surface.

MATERIALS AND METHODS

Study Design

An established acute ventral hernia model, previously described, was used for this study.[13,14,15,16,17,18,19,20,21] Fifty-six Hartley guinea pigs (460–500 g) underwent bridged ventral hernia repair with inlay HADM (AlloDerm “thick” [0.79–1.79 mm thick], LifeCell Corporation, Branchburg, NJ) oriented with the BM toward or away from the peritoneal cavity. At postoperative week 1, 2, or 4, the guinea pigs were killed and abdominal wall repairs excised. Histologic and immunohistochemical analyses were performed to quantify cellular and vascular density within distinct zones of the repair-site cross-sections. Subgroup analyses were performed to identify the quantity of cellular and vascular infiltration as a function of time after implantation, BM orientation, and tissue type directly adjacent to the HADM.

Surgical Technique

Guinea pigs were anesthetized with buprenorphine (0.05mg/kg intramuscularly [IM]), ketamine (25–50mg/kg IM), and xylazine (2.5–5mg/kg IM). Intraoperatively, animal received continuous inhaled oxygen (2L/min) and isoflurane (0.5–2%). Each animal received antibiotic prophylaxis (enrofloxacin, 5mg/kg IM) preoperatively and daily for 2 days. The animals’ abdominal walls were shaved, prepared with chlorhexidine, and draped sterilely.

A 4-cm midline incision was made between the xiphoid and the pubis, and a 3- × 1-cm fascial defect was created to expose the peritoneal cavity. An elliptically shaped HADM implant (4 × 2 cm of AlloDerm) was created from a sterile template after appropriate

rehydration. HADM was implanted with the BM facing either toward the peritoneum (BM in; n=39) or toward the subcutaneous tissue (BM out; n=19). An inlay bridge technique secured the mesh to the musculofascial defect using a 5-0 running polypropylene suture. The repair resulted in 0.5-cm of musculofascia-bioprosthesis overlap circumferentially. Absorbable dermal sutures and skin clips were used to close the skin.

Animals were evaluated daily for hernia recurrence and complications, such as hematoma, seroma, or skin dehiscence. At week 1, 2, or 4, the animals were killed by carbon dioxide asphyxiation. The entire abdominal wall, including the repair site, was excised. After gross observations were made, transverse, full-thickness tissue samples were harvested from each repair site and included 1-cm of muscle/skin on each side.

Histologic and Immunohistochemical Analysis

Tissue samples were fixed in 10% formalin and paraffin embedded. Sections (4 μm thick) were cut and stained with hematoxylin-eosin stain (H&E) to assess cellular infiltration and with anti-factor VIII antibodies for vascular infiltration.

Mesh cross-sections were divided into three distinct zones as shown in Fig. 1: the interface zone (HADM dorsal to and directly contiguous with the musculofascial defect edge), the central zone (HADM in the "bridging" area directly beneath the subcutaneous fat), and the junction zone (area between the interface zone and center zone). The junction zone represents a ‘spacer’ separating the two main zones of interest, the interface with muscle adjacent and the center with fat adjacent. This was done to ensure that no partial effect of these adjacent tissues was tabulated. Each zone was further divided into two equally thick halves: one facing inward toward the peritoneal cavity and the other toward the subcutaneous tissues. The subzones were thus the interface-surface (IS) and interface-peritoneum (IP) subzones, the center-surface (CS) and center-peritoneum (CP) subzones, and the junction-surface (JS) and junction-peritoneum (JP) subzones. Each subzone was approximately 0.33cm wide by 1.29mm. Imaging of stained slides was done with a Retiga 4000R digital camera (QImaging, Surrey, British Columbia) mounted on an Olympus IX70 inverted microscope (Olympus, Melville, NY). Cells and vessels were counted in each subzone of each cross-section of each repair under high power (200×) magnification in a blinded fashion and expressed as cells or vessels per mm^2. Cellular infiltration was determined only within the HADM itself; cells surrounding the HADM were not counted. Cells were defined as having a basophilic nucleus with eosinophilic cytoplasm, and vessels were defined as circular structures lined with an endothelium staining positively for factor VIII. Images were analyzed with ImageJ 1.32j software (National Institutes of Health, Bethesda, MD).

Statistical Analysis

Cellular and vascular infiltration data was collected within all bioprosthesis subzones (IS, IP, CS, CP, JS, and JP). With mesh attached to musculofascia on both sides of the bridged defect, there were two interface zones and two junction zones (but only one center zone) per cross-section.

A mixed effect linear model was fitted to both cell and vessel data (MIXED procedure, SAS version 9.2 software, SAS Institute Inc., Cary, NC).[22] Fixed effects included postoperative week, zone, BM orientation, and BM orientation by zone interaction. A random effect was also included with a compound symmetry variance-covariance structure to account for the natural correlated structure of the within-subject repeated measures. Comparisons were made between the interface (IP+IS), junction (JS+JP), and center (CS+CP) zones and between all surface (IS+JS+CS) and peritoneal (IP+JP+CP) subzones. The surface and

peritoneal sides of mesh, including both BM in and out data for each was evaluated to isolate potential differences in cellular and vascular infiltration between mesh surface and peritoneal sides with BM orientation as a fixed effect. BM orientation was then evaluated separately with other variables, such as zone and week, maintained as fixed effects, to isolate differences in cellular and vascular infiltration unique to BM orientation.

The relative tissue source contributions to infiltration were evaluated for the interface zone as compared to the center zone for BM in at each week, as well as BM out at each week. The role of the BM itself was further evaluated by comparing BM in versus out for the surface side and also peritoneal side infiltration at each week. BM in versus out was also compared separately for the interface and center zones at each week. All comparisons within the fixed effects were accomplished with linear contrasts and based on F-tests.

Statistical models and comparisons were performed by a senior biomedical statistician (J.E.). Cellular and vascular densities are reported as means with standard deviations. Statistical significance was defined as values of $p < 0.05$.

RESULTS

Surgical Outcomes

Animal survival was 100%. No wound infections, seromas, eviscerations, recurrent hernias, visceral perforations, bowel obstructions, or enterocutaneous fistulas occurred. No bowel adhesions to repair sites were seen in any animal. Auto-cannibalism suture removal resulted in a minor (<0.5-cm) skin dehiscence in one animal; this healed fully without intervention within 4 days.

Cellular Infiltration

Postoperative Week—Cellular infiltration into HADM increased over time in all areas. The mean density of cells was significantly greater at week 4 than week 1 (290±49 vs. 50±49, respectively, p=0.02).

Zone—Mean cell density was greater in the interface than center at weeks 1 and 2 [120±16 vs. 82±21 cells/mm^2 (p=0.01); 360±36 vs. 220±44 cells/mm^2 (p<0.0001), respectively] (Fig 2). No significant difference in cell density was observed at week 4 between the interface and center zones [560±45 vs. 570±62 cells/mm^2 (p=0.8), respectively], perhaps owing to penetration of cells into all areas of the mesh by this time (Fig. 2).

For the BM in orientation, the interface demonstrated greater cellular infiltration than the center at week 1 and 2 [64±44 vs. 43±33 cells/mm^2 (p=0.048); 170±100 vs. 110±100 cells/mm^2 (p=0.0010), respectively]. For the BM out orientation, the interface demonstrated greater cellular infiltration than the center at week 2 [180±110 vs. 110±37 cells/mm^2 (p=0.02)].

The side of the mesh facing the surface (subcutaneous fat or muscle) demonstrated greater mean cell density than the side facing the peritoneum at weeks 1 and 2 [190±26 vs. 120±26 cells/mm^2 (p=0.001); 470±60 vs. 360±58 cells/mm^2 (p=0.005), respectively]. . By 4 weeks, though, the sides exhibited no difference in cell density [850±76 vs. 860±76 cells/mm^2 (p=0.88)]. This also was likely due to cellular infiltration into all areas by 4 weeks.

For the BM in orientation, cellular infiltration was significantly greater for the surface side than peritoneal at week 1 and 2 [70±40 vs. 40±50 cells/mm^2, p=0.0009; 150±110 vs. 120±100 cells/mm^2, p=0.0013, respectively]. No significant differences were observed with

the BM out orientation, perhaps related to the BM inhibiting cellular infiltration from the surface-side musculofascial edge.

BM Orientation—Representative images of cellular infiltration at week 4 with the BM in and out are shown in Fig. 3. The BM appeared to inhibit cellular infiltration at week 4 but not at earlier time points (Fig. 4). At weeks 1 and 2, no significant difference was seen in mean cell density regardless of whether the BM was oriented toward or away from the peritoneum [52±16 vs. 51±21 cells/mm^2 (p=0.9); 130±12 vs. 150±20 cells/mm^2 (p=0.5), respectively] (Fig.4) . At 4 weeks, however, greater mean cell density was evident when the BM was oriented toward the peritoneum [310±13 for BM in vs. 260±17 cells/mm^2 for BM out (p=0.02)] (Fig.4)), consistent with the observation that the BM inhibits cellular infiltration, most of which is from the muscle edge.

Additional evaluation of cellular infiltration within the fixed effects for BM in versus out at the surface and peritoneal sides was performed at each week. There were significantly more cells for BM in than out at week 4 on the surface side (320±120 BM in vs. 230 ± 150 cells/mm^2, p=0.025). .

Vascular Infiltration

Postoperative Week—Vascular infiltration increased over time in all areas. The mean vessel density was significantly greater at week 4 (9±3 vessels/mm^2) than week 1 (2±3 vessels/mm^2, p=0.001).

Zone—Greater mean vessel density was seen in the interface than the center zone at week 4 [23±2 vs. 15±2 vessels/mm^2 (p<0.0001)] (Fig. 5)). The mean vessel density was greater in the interface compared to center zone at weeks 1 and 2, but insignificant (Fig. 5).

Additional evaluation within the fixed effects of the interface versus center zones for vascular infiltration revealed that for BM in, there was a significantly greater number of vessels at the interface zone at all time points with statistical significance seen at week 4 (14±7 vs. 9±4 vessels/mm^2, p=0.<0.0001) . For BM out, there was consistently greater vascular infiltration at each week, reaching significance at week 4 (8±4 vs. 5±4 vessels/mm^2, p=0.022).

Unlike cell density at weeks 1 and 2, vessel density did not differ between the surface and peritoneal sides of the mesh at any time point. Further analysis of the surface compared to peritoneal sides of mesh demonstrated that there was no difference in vascular infiltration at any time point.

BM Orientation—Representative images showing vascular infiltration at week 4 for BM-in and BM-out orientations are shown in Fig. 6. The BM appeared to inhibit vascular infiltration when placed outward toward the muscle and subcutaneous fat. At week 2, there was a non-significant trend toward greater vessel density when the BM was placed toward vs. away from the peritoneum [7±1 vs. 4±1 vessels/mm^2, respectively (p=0.06)]. At week 4, significantly greater mean vessel density was seen with the BM-in orientation compared to the BM-out orientation [12±1 vs. 7±1 vessels/mm^2 (p=0.0004)] (Fig. 7).

Further comparisons of the BM in versus out for the surface and peritoneal sides at each week within the fixed effects using linear contrasts showed that the BM in orientation had greater vascular infiltration at both the surface and peritoneal sides at each week (Table 6). The difference was significant at week 1 and 4 for the surface side (3±4 vs. 1±1 vessels/mm^2, p=0.028; 12±6 vs. 7±6 vessels/mm^2, p=0.014) and at week 4 for the peritoneal side (12±7 vs. 6±4 vessels/mm^2, p=0.0029). This is consistent with the proposition that the BM,

when oriented as to block the main source of vessel infiltration into mesh (the interface zone, musculofascia, in our data), acts to inhibit vascular infiltration.

DISCUSSION

The metrics of cellular and vascular infiltration into implanted bioprosthetic mesh have not been described in abdominal wall reconstruction, to our knowledge. Using an established ventral hernia model [13–21] and HADM, the bioprosthetic mesh whose clinical use has been most extensively reported, we addressed several previously unknown aspects of bioprosthetic mesh remodeling in the first 4 weeks after implantation. In this study, cellular and vascular infiltration into HADM used for ventral hernia repair increased over time in all mesh areas. In general, the interface zone (adjacent to musculofascia) demonstrated greater infiltration than the center zone (adjacent to subcutaneous fat). Subcutaneous fat did, however, contribute to cellular and vascular infiltration into mesh. These findings improve our understanding of bioprosthetic mesh remodeling; may direct the development of new, optimized biologic implants; and are directly translatable into clinical practice. The findings support the hypothesis that the musculofascial edge provides the most significant source of cells and vessels, and that the BM inhibits penetration of cells and vessels into HADM. This suggests that bioprosthetic mesh should overlap the musculofascia as much as possible and that the BM (if present in the bioprosthesis) should be oriented to face the surface believed to be least likely to produce cellular and vascular infiltration. Surgeons may also choose to minimize the size of any fascial defect bridged with bioprosthetic mesh, including the use of component separation techniques. The finding that subcutaneous fat is a good source of vascular and cell in-growth is clinically relevant to patient management. The central portion of a bridged repair is remote from the musculofascial edges, but cells and vessels from the overlying subcutaneous fat penetrate the bioprosthetic mesh providing host tissue incorporation. Thus, even in large bridged repairs the entire surface area of bioprosthetic mesh becomes vascularized and incorporated with cells. Surgeons may feel more comfortable managing a mesh exposure from skin separation and/or a localized bacterial infection conservatively rather than debriding or explanting the mesh assuming that it is unlikely to become vascularized.

We observed that by 4 weeks, the BM significantly inhibited both cellular and vascular infiltration into HADM. To achieve maximal neovascularization within the bioprosthesis, therefore, the BM should be oriented inward toward the peritoneum in ventral hernia repair, allowing maximum infiltration of cells and vessels from the musculofascia and subcutaneous fat. To optimally remodel bioprosthetic mesh into host tissue without stretch or loss of mechanical strength there needs to be a delicate balance between collagen degradation and deposition. The rate of cell and vessel infiltration may influence this balance. Although maximum cell and vascular infiltration rates are likely favorable for mesh-interface incorporation strength and resistance to bacterial infection there may be adverse consequences to the material’s mechanical strength if cell and vascular infiltration is too rapid.

Although not evaluated, BM orientation may also be important when using HADM for implant-based breast reconstruction. These data provide at least theoretic support for placing the BM surface toward the breast implant rather than the mastectomy skin flaps to optimize remodeling when used for breast reconstruction. Further studies will elucidate specific quantitative differences in cellular and vascular infiltration, if they exist, for this application.

A strength of this study is the established nature of the ventral hernia model. This model has yielded consistent results in multiple studies and therefore is reliable. Another strength is the use of a mixed effects linear model for complex statistical analysis, which allows evaluation

of each study variable (time, mesh zone, and BM orientation).. This study was limited by its use of HADM only; however, HADM has been the most widely used and studied bioprosthetic material. Other bioprosthetic materials are produced from human and xenogeneic source tissues and may not contain an intact BM. Though assumed to be related to mechanical blockade, the mechanisms by which the BM seems to impede cellular and vascular infiltration from musculofascia and subcutaneous fat were not elucidated. We also did not differentiate cell types, instead quantifying cellular infiltration from different tissue sources (musculofascia and subcutaneous fat) and with different BM orientations. Future studies will help evaluate specific types of infiltrating cells.

This study fills gaps in understanding bioprosthetic mesh remodeling. These findings may be immediately translated into clinical practice and may improve our knowledge of the biologic behavior of bioprosthetic implants.

CONCLUSION

Cellular and vascular infiltration into HADM was found to be greater from the musculofascia than from subcutaneous fat, even though the subcutaneous fat was a robust contributor to both. The BM surface appeared to inhibit cellular and vascular infiltration by 4 weeks; therefore, in clinical ventral hernia repairs, orienting the BM surface toward the peritoneal cavity may improve host remodeling of the implanted bioprosthetic mesh. Further studies will be helpful to evaluate additional aspects of bioprosthetic mesh remodeling including longer-term outcomes, different bioprosthetic mesh materials, and the specific distribution of infiltrating cell types over time.

Acknowledgments

Financial support: This work was funded in part by a grant from the Plastic Surgery Education Foundation (BRG63-08), a sponsored research grant from LifeCell Corporation and the National Institutes of Health (RAG026477-01A2). MD Anderson is supported in part by a Cancer Center Support Grant (CA16672) from the National Institutes of Health.

REFERENCES

1. Milburn ML, Holton LH, Chung TL, Li EN, Bochicchio G, Goldberg NH, Silverman RP. Acellular dermal matrix compared with synthetic implant material for repair of ventral hernia in the setting of peri-operative Staphylococcus aureus implant contamination: a rabbit model. Surg Infect (Larchmt). 2008; 9(4):433–442. [PubMed: 18759680]
2. Sandor M, Xu H, Connor J, Lombardi J, Harper JR, Silverman RP, McQuillan DJ. Host response to implanted porcine-derived biologic materials in a primate model of abdominal wall repair. Tissue Eng Part A. 2008; 14(12):2021–2031. [PubMed: 18657025]
3. Wu X, Kathuria N, Patrick CW, Reece GP. Quantitative analysis of the microvasculature growing in the fibrin interface between a skin graft and the recipient site. Microvasc Res. 2008; 75(1):119–129. [PubMed: 17631360]
4. Eppley B. Experimental assessment of the revascularization of acellular human dermis for soft-tissue augmentation. Plast Reconstr Surg. 2001; 107(3):757–762. [PubMed: 11304602]
5. Menon N, Rodriguez ED, Byrnes CK, Girotto JA, Goldberg NH, Silverman RP. Revascularization of human acellular dermis in full-thickness abdominal wall reconstruction in the rabbit model. Ann Plast Surg. 2003; 50(5):523–527. [PubMed: 12792544]
6. Breuing KH, Warren SM. Immediate bilateral breast reconstruction with implants and inferolateral AlloDerm slings. Ann Plast Surg. 2005; 55(3):232–239. [PubMed: 16106158]
7. Buinewicz B, Rosen B. Acellular cadaveric dermis (AlloDerm): a new alternative for abdominal hernia repair. Ann Plast Surg. 2004; 52(2):188–194. [PubMed: 14745271]

8. Butler CE, Langstein HN, Kronowitz SJ. Pelvic, abdominal, and chest wall reconstruction with AlloDerm in patients at increased risk for mesh-related complications. Plast Reconstr Surg. 2005; 115(5):1276–1277.
9. Misra S, Raj PK, Tarr SM, Treat RC. Results of AlloDerm use in abdominal hernia repair. Hernia. 2008; 12(3):247–250. [PubMed: 18209948]
10. Nahabedian M. AlloDerm performance in the setting of prosthetic breast surgery, infection, and irradiation. Plast Reconstr Surg. 2009; 124(6):1743–1753. [PubMed: 19952629]
11. Sacks JM, Butler CE. Outcomes of Complex Abdominal Wall Reconstruction with Bioprosthetic Mesh in Cancer Patients. Plast Reconstr Surg. 2008; 121(6S):39.
12. Spear SL, Parikh PM, Reisin E, Menon NG. Acellular dermis-assisted breast reconstruction. Aesthetic Plast Surg. 2008; 32(3):418–425. [PubMed: 18338102]
13. Butler CE, Navarro FA, Orgill DP. Reduction of abdominal adhesions using composite collagen-GAG implants for ventral hernia repair. Journal of Biomedical Materials Research. 2001; 58(1): 75–80. [PubMed: 11153001]
14. Butler CE, Prieto VG. Reduction of adhesions with composite AlloDerm/polypropylene mesh implants for abdominal wall reconstruction. Plast Reconstr Surg. 2004; 114(2):464–473. [PubMed: 15277815]
15. Gobin A, Butler CE, Mathur AB. Repair and regeneration of the abdominal wall musculofascial defect using silk fibroin-chitosan blend. Tissue Eng. 2006; 12(12):3383–3394. [PubMed: 17518675]
16. Burns NK, Rios CN, Jaffari MV, Mathur AB, Butler CE. Ventral Hernia Repair with Porcine vs. Human Acellular Dermal Matrices. J Am Coll Surg. 2008; 207(3):S66–S67.
17. Burns NK, Jaffari MV, Rios CN, Mathur AB, Butler CE. Non-cross-linked porcine acellular dermal matrices for abdominal wall reconstruction. Plast Reconstr Surg. 2010; 125(1):167–176. [PubMed: 19910855]
18. Campbell KT, Burns NK, Rios CN, Mathur AB, Butler CE. In Vivo Comparison of Human Acellular Dermal Matrix and Non-Cross-Linked Porcine Acellular Dermal Matrix. Plast Reconstr Surg. 2010; 125(6S):111. [PubMed: 19770815]
19. Butler CE, Burns NK, Turza Campbell K, Mathur AB, Jaffari MV, Rios CN. Comparison of Cross-Linked and Non-Cross-Linked Porcine Acellular Dermal Matrices for Ventral Hernia Repair. J Am Coll Surg. 2010; 211(3):368–376. [PubMed: 20800194]
20. Turza Campbell K, Burns NK, Rios CN, Mathur AB, Butler CE. Human versus Non-cross-linked porcine acellular dermal matrix used for ventral hernia repair: Comparison of in vivo fibrovascular remodeling and mechanical strength. Plast Reconstr Surg. 2010; 127(6):2321–2332.
21. Turza Campbell K, Burns NK, Butler CE. Evaluation of Human Acellular Dermal Matrices for the Metrics of Cellular and Vascular Infiltration. Plast Reconstr Surg. 2010; 126(4S):85–86.
22. Brown, H.; Prescott, R., editors. Applied Mixed Models in Medicine. 2nd edition. New York: John Wiley & Sons; 1999.

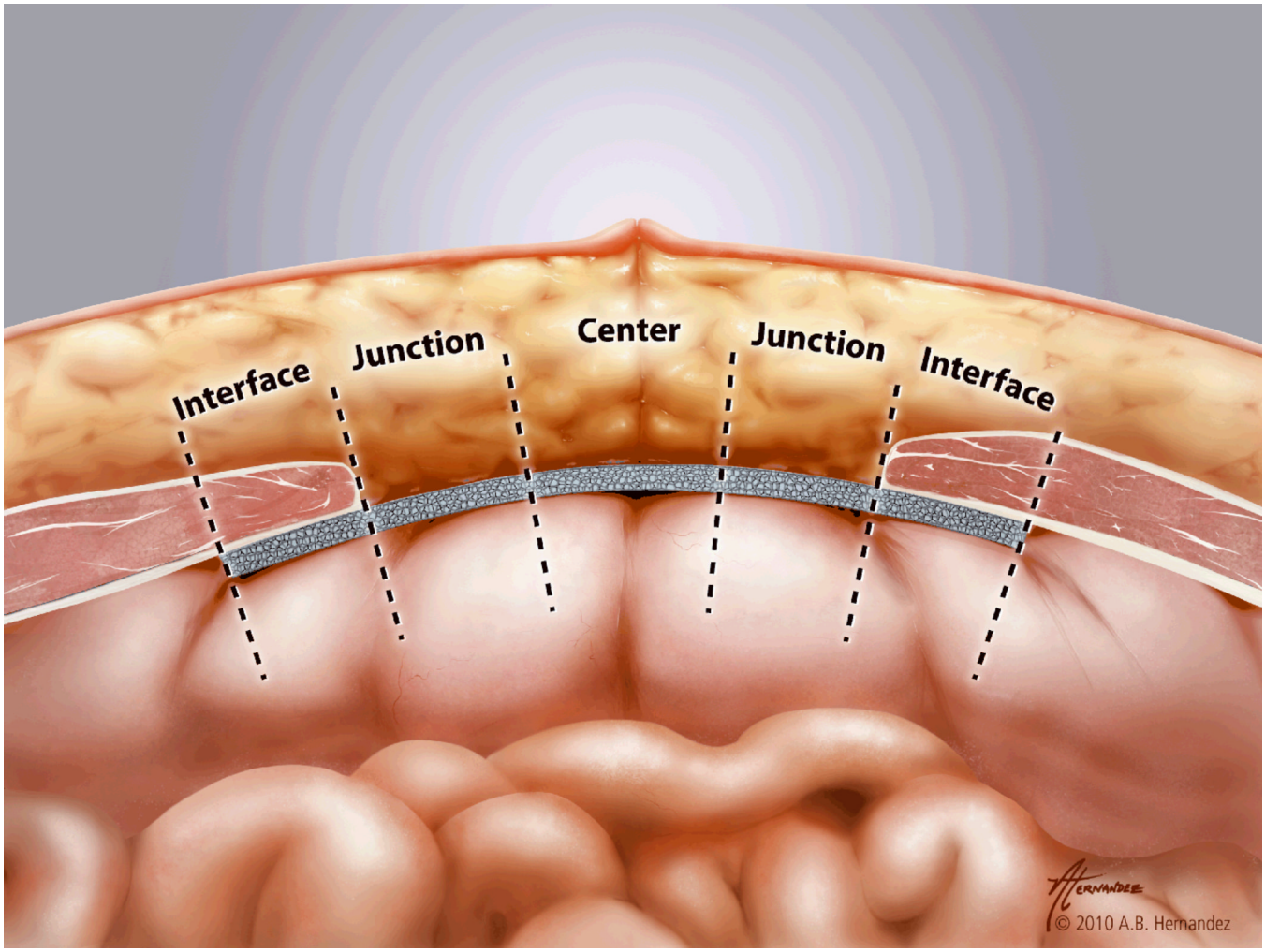

Figure 1.
Bioprosthetic zone diagram demonstrating the interface zone (HADM dorsal to and directly contiguous with the musculofascial defect edge), the central zone (HADM in the "bridging" area directly beneath the subcutaneous fat), and the junction zone (area between the interface zone and center zone).

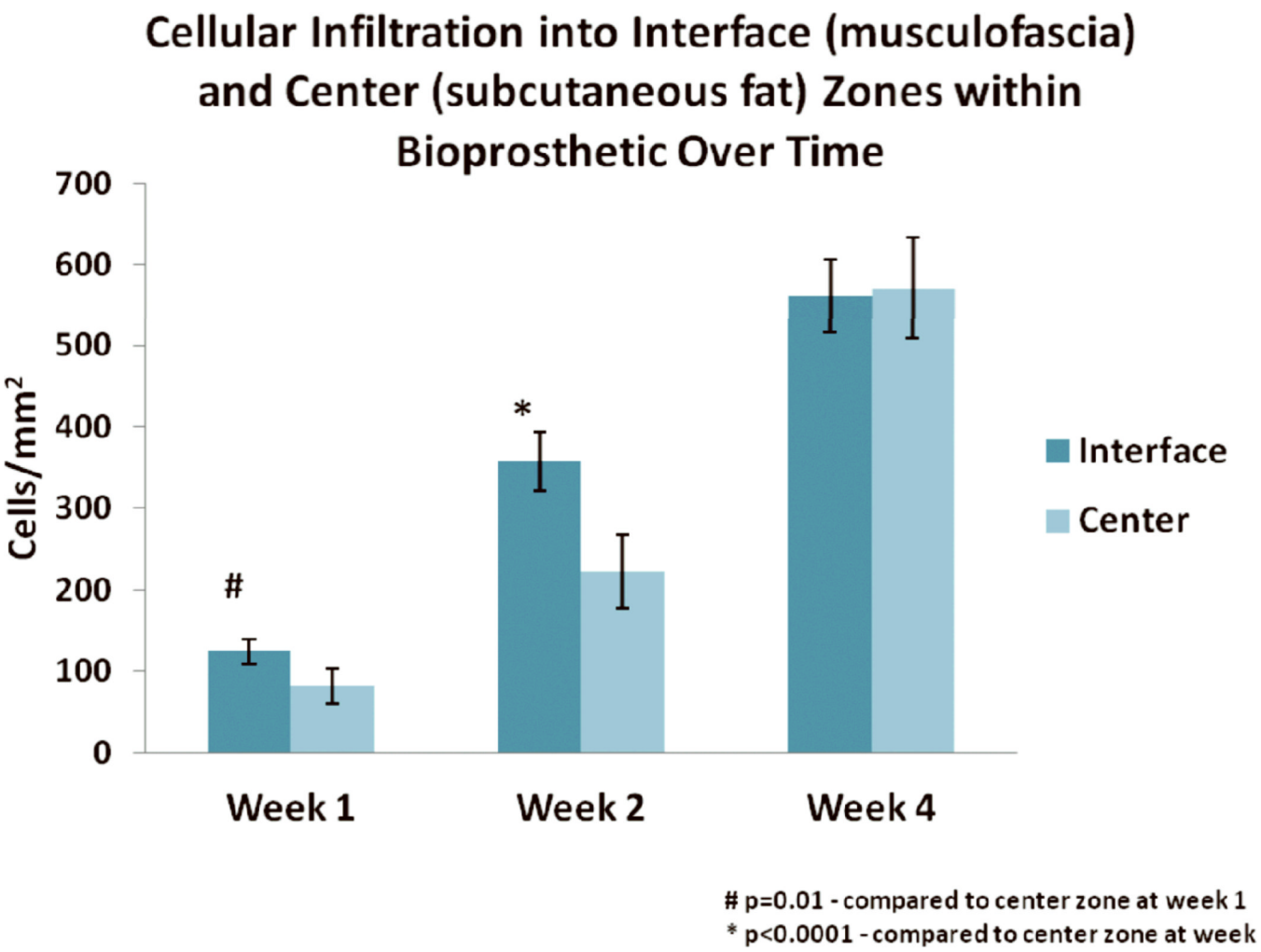

Figure 2.

Mean cell density (± standard deviation) in the interface and center zones of implanted HADM over time. # indicates p=0.01 for interface zone compared to center at week 1. * indicates p<0.0001 for interface compared to center at week 2.

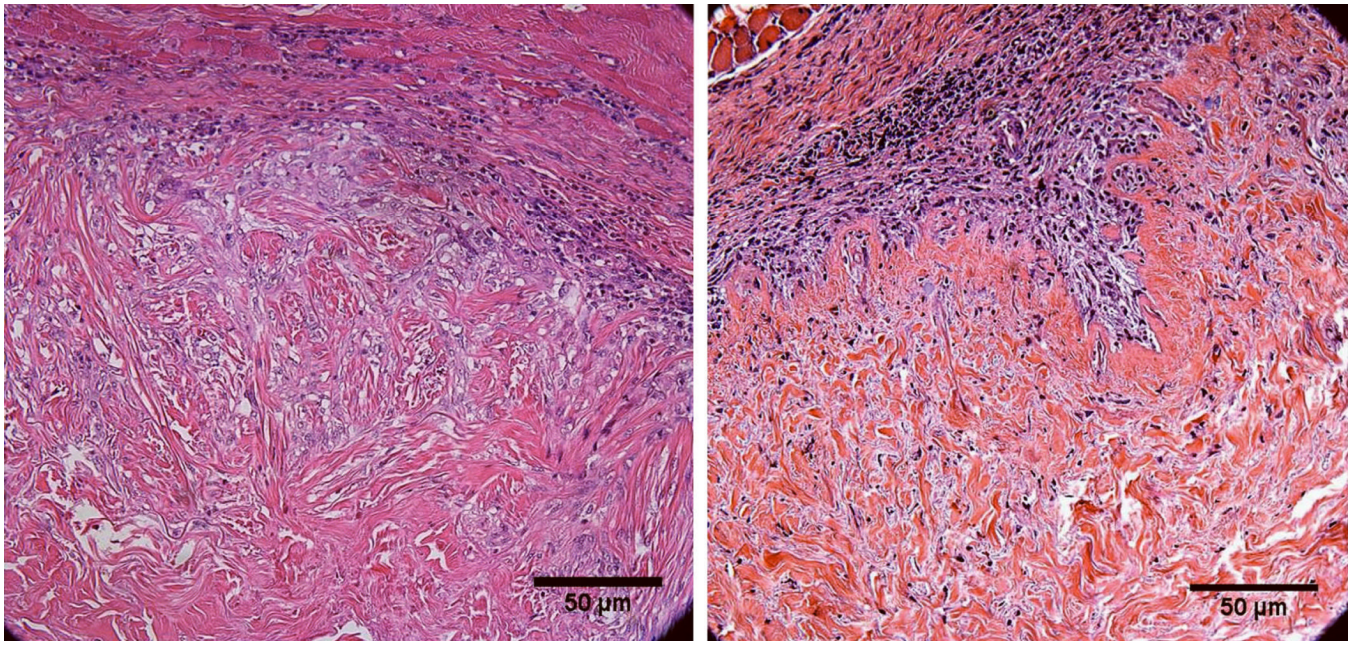

Figure 3.
Representative H&E-stained images at week 4 showing greater cellular infiltration into HADM implanted with the BM in (left) versus the BM out (right).

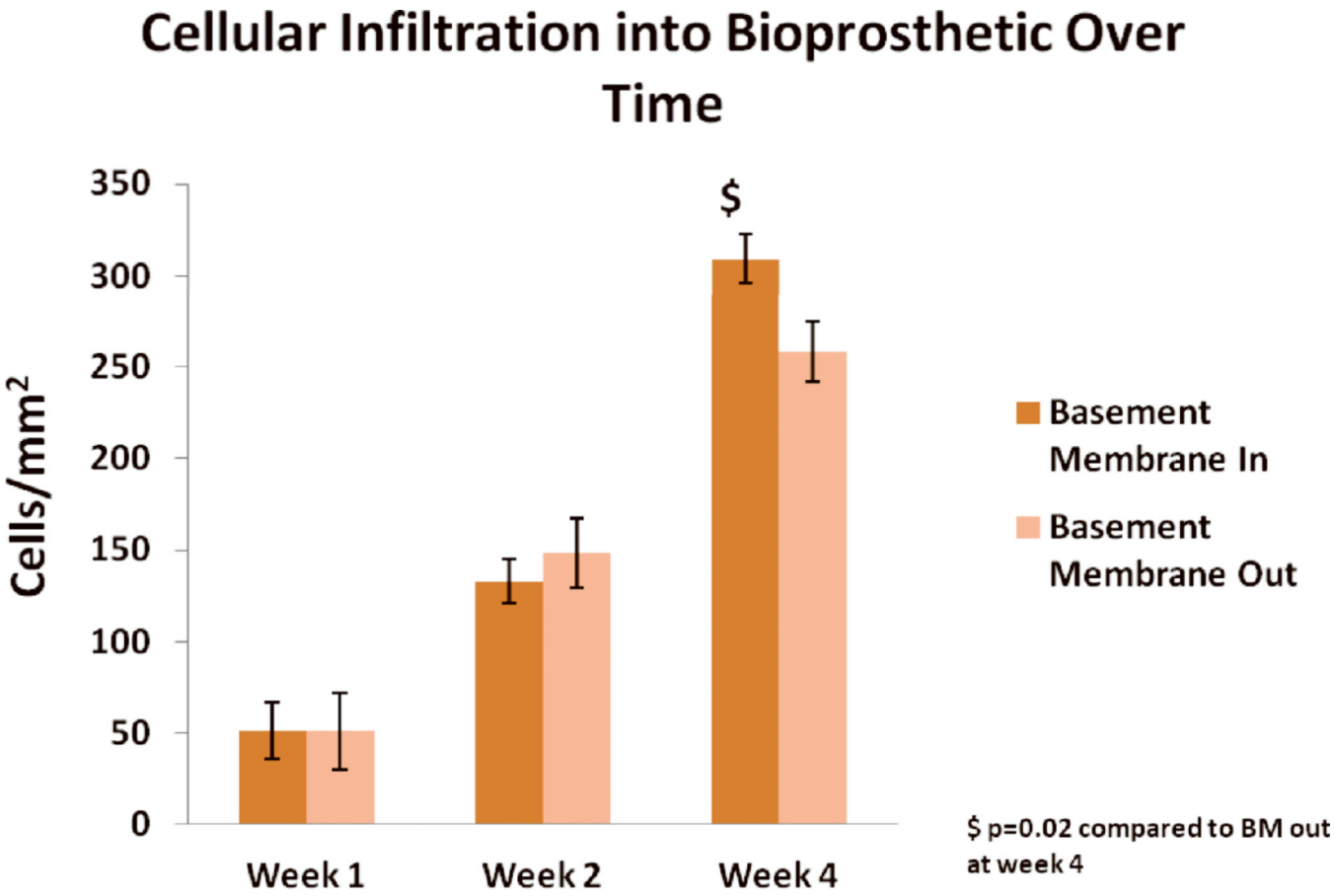

Figure 4.
Mean cell density (± standard deviation) in HADM implanted with BM in versus BM out over time. $ indicates p=0.02 for BM in compared to out at week 4.

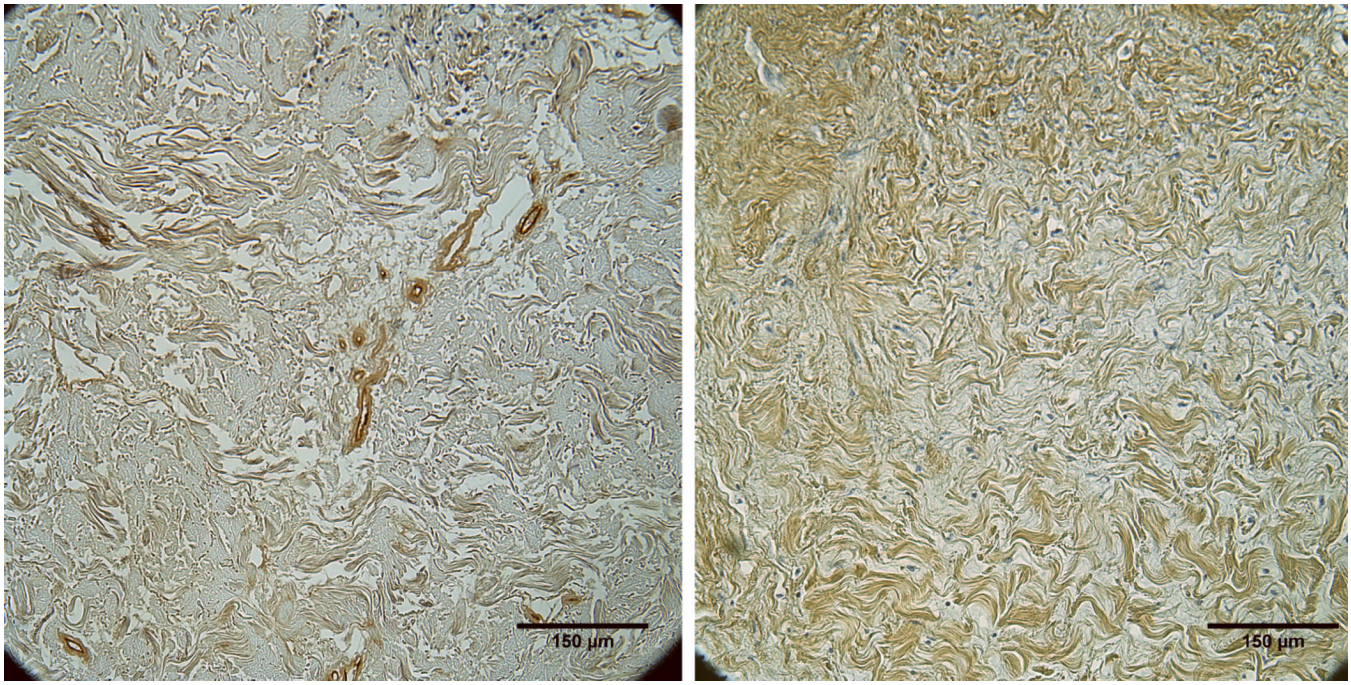

Figure 5.
Mean vessel density (± standard deviation) in the interface versus center zones of implanted HADM over time. * indicates $p<0.0001$ interface zone compared to center zone at week 4.

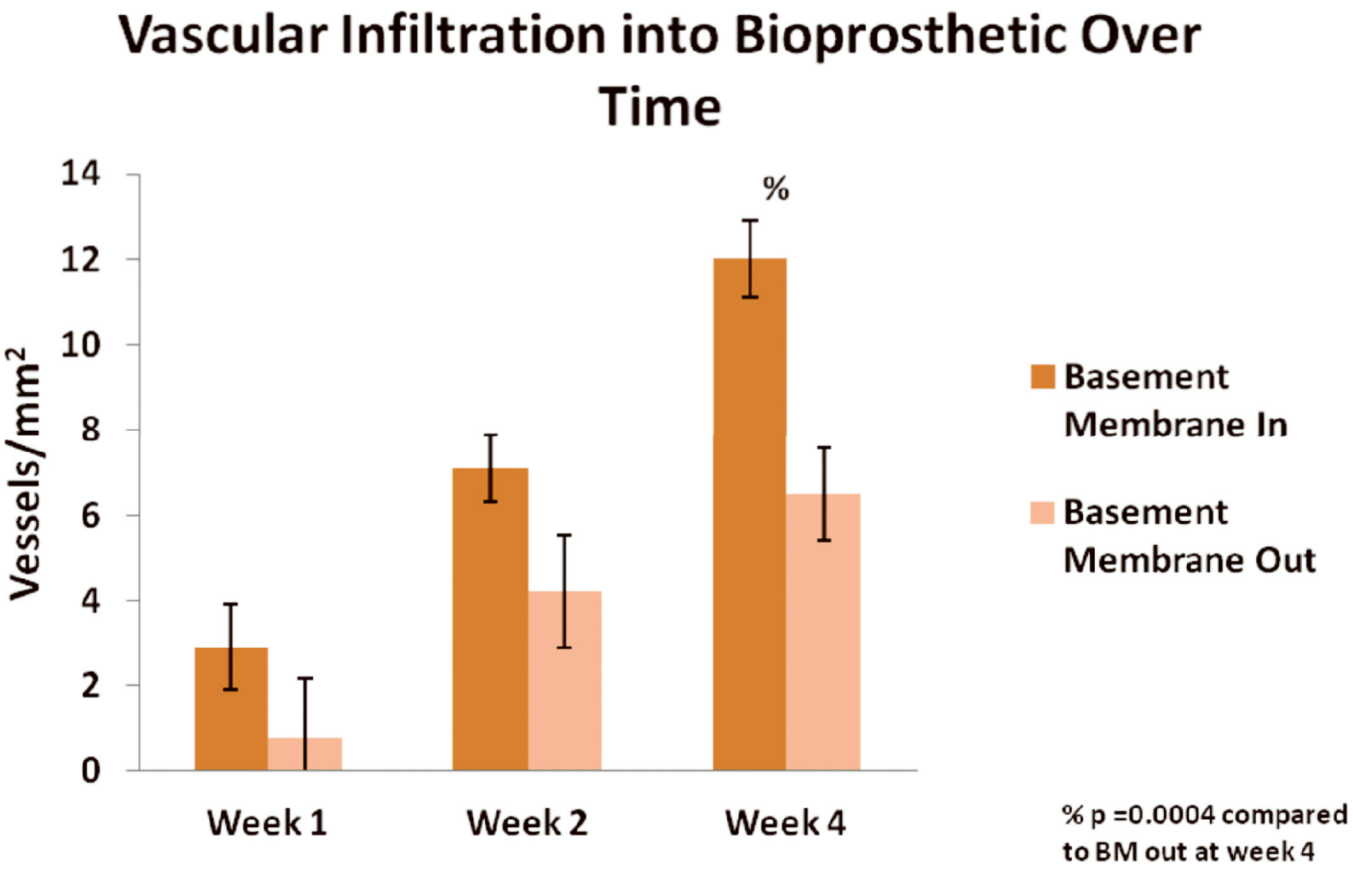

Figure 6.
Representative images stained for factor VIII showing greater vascular infiltration into HADM implanted with the BM in (left) versus the BM out (right) at week 4.

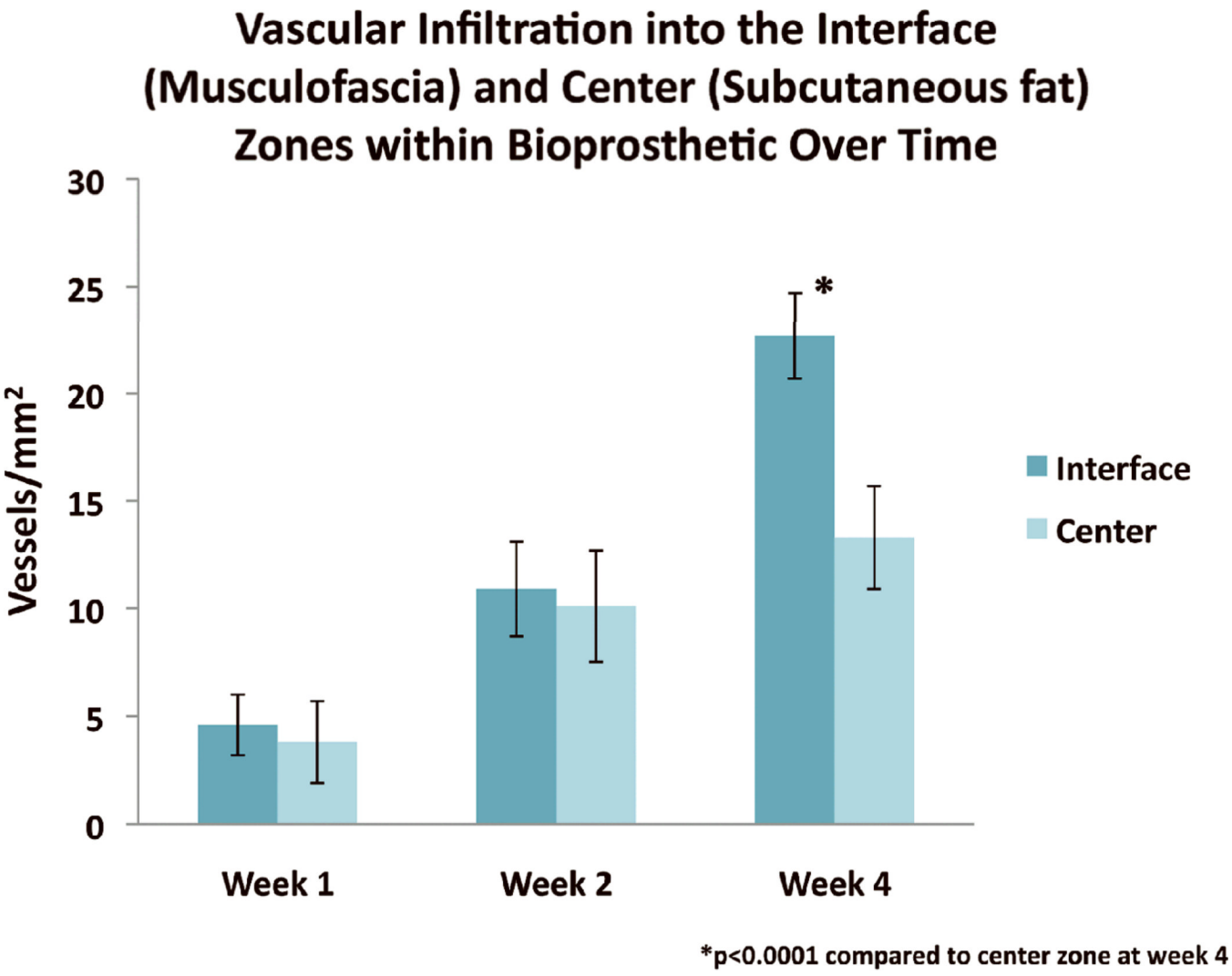

Figure 7.
Mean vascular density (± standard deviation) in HADM implanted with the BM in versus BM out over time. % indicates p=0.0004 for BM in compared to BM out at week 4.